EFDA–JET–PR(11)48

F. Durodié, M.P.S. Nightingale, M.-L. Mayoral, J. Ongena, A. Argouarch, G. Berger-By, T. Blackman, V. Cocilovo, A. Czarnecka, S. Dowson, D. Frigione, R. Goulding, M. Graham, J. Hobirk, S. Huygen, S. Jachmich, P. Jacquet, E. Lerche, P.U. Lamalle, T. Loarer, R. Maggiora, A. Messiaen, D. Milanesio, I. Monakhov, M.F.F. Nave, F. Rimini, H. Sheikh, C. Sozzi, M. Tsalas, D. Van Eester, M. Vrancken, A. Whitehurst, E. Wooldridge, K.-D. Zastrow and JET EFDA contributors

Operational Experience with the ICRF ITER Like Antenna on JET

Operational Experience with the ICRF ITER Like Antenna on JET

F. Durodié[1], M.P.S. Nightingale[2], M.-L. Mayoral[2], J. Ongena[1], A. Argouarch[3], G. Berger-By[3], T. Blackman[2], V. Cocilovo[4], A. Czarnecka[5], S. Dowson[2], D. Frigione[4], R. Goulding[7], M. Graham[2], J. Hobirk[6], S. Huygen[1], S. Jachmich[1], P. Jacquet[2], E. Lerche[1], P.U. Lamalle[1], T. Loarer[3], R. Maggiora[8], A. Messiaen[1], D. Milanesio[8], I. Monakhov[2], M.F.F. Nave[9], F. Rimini[10], H. Sheikh[2], C. Sozzi[11], M. Tsalas[12], D. Van Eester[1], M. Vrancken[1], A. Whitehurst[2], E. Wooldridge[2], K.-D. Zastrow[2] and JET EFDA contributors*

JET-EFDA, Culham Science Centre, OX14 3DB, Abingdon, UK

[1]LPP-ERM/KMS, Association "EURATOM-Belgian State", 1000 Brussels, Belgium, TEC Partner
[2]EURATOM/CCFE Fusion Association, Culham Science Center, Abingdon, OX14 3DB, UK.
[3]Institut pour les Recherches en Fusion Magnétique, CEA-Cadarache, F-13108 Saint-Paul-lez-Durance, France.
[4]Associazione EURATOM-ENEA sulla Fusione, C.R. Frascati, Roma, Italy.
[5]Association EURATOM-IPPLM, Hery 23, 01-497, Warsaw, Poland.
[6]Max-Planck-Institut für Plasmaphysik, EURATOM-Assoziation, D-85748 Garching, Germany
[7]Oak Ridge National Laboratory, Oak Ridge, United States
[8]Institute Politechnico di Turin, Torino, Italy
[9]Associação EURATOM/IST, Instituto de Plasma e Fusão Nuclear, 1049-001 Lisbon, Portugal
[10]EFDA Close Support Unit, Culham Science Center, Culham, OX14 3DB, UK
[11]Istituto di Fisica del Plasma CNR, EURATOM-ENEA-CNR Association, Milano, Italy
[12]Association EURATOM-Hellas, NCSR "Demokritos", Agia Paraskevi Attica, Greece
** See annex of F. Romanelli et al, "Overview of JET Results",*
(23rd IAEA Fusion Energy Conference, Daejon, Republic of Korea (2010)).

Preprint of Paper to be submitted for publication in
Plasma Physics and Controlled Fusion

ABSTRACT.
The paper summarizes the operational experience of the Ion Cyclotron Range of Frequencies (ICRF) ITER Like Antenna (ILA) on JET aiming at substantially increasing the power density in the range of the requirements for ITER combined with load resiliency. An in depth description of its commissioning, operational aspects and achieved performances are presented.

1. INTRODUCTION

The capability of Ion Cyclotron Resonance Frequency (ICRF) systems to reliably couple large amounts of power to ELMy H-mode plasmas is essential for both the JET research program and the future use of such systems on ITER and fusion reactors based on magnetic confinement. To make this possible, several key issues with ICRF systems needed to be addressed:

- Power densities on present day experiments on ELMy H-mode plasmas were typically lower than needed for ITER and fusion reactor applications where the available wall surface that can be dedicated to plasma heating systems is competing with blanket modules for breeding tritium.
- In order to achieve high power densities, reliable operation at high voltages must be demonstrated.
- The modelling of the RF coupling must be validated to allow predictive design ICRF launcher for ITER.
- The impurity production due to RF sheaths must be minimized : in the context of the ILA project the dependency on the power density must be assessed.
- The RF system must be tolerant to plasma coupling variations such as these resulting of Edge Localized Modes (ELMs) producing strong, fast and frequent antenna loading perturbations (up to a 10-fold load increase in less than 100ms), which force RF power generators to temporarily cut out (trip) thereby substantially reducing the average RF power that is coupled to the plasma.

These problems were addressed in JET by the installation of a new system based on a new design approach, the ITER Like Antenna (ILA). The operational experience with this new antenna, which was installed along side the existing ICRF Antennas retrofitted with load tolerant feeding transmission line circuits [1], will be described in detail in the following sections.

2. THE JET ITER-LIKE ANTENNA

The ITER Like Antenna project (ILA) [2, 3] consists in a compact design of the conjugate-T approach [4, 5] featuring in-vessel matching capacitors to achieve the desired T-junction impedance (Fig.1a, 1b and 1.c). It is closely related to the former baseline option for ITER described in the 1998 DDD [6]. The Conjugate-T (CT) concept is an evolution of the Resonant Double Loop (RDL) concept [7] and consists of pairs of straps each with an adjustable impedance transformation (series capacitor in the case of the ILA, parallel stub or, as in the case of the External Conjugate-T [8, 9], a variable

length transmission line) fed from a common T-junction. Matching is achieved by adjusting these variable impedance transformers such that the two branches have complex conjugate admittances at the Tjunction (where they are connected in parallel, hence the name of this technique). This eliminates the branch susceptibilities and only the sum of the branch conductances remains. The target impedance at the CT, Z_{CT}, can be chosen for a reference plasma loading condition to minimize the variations of ZCT to plasma load variations due to e.g. ELMs (see Fig.2). This target impedance is typically between 3 and 6Ω, thus much lower than the characteristic impedance of transmission lines, Z_0 (at JET $Z_0 = 30$). For asymmetric straps (either due to geometry or due to plasma effects) the Z_{CT} can have a small reactive part in order to equalize the branch voltages. A "fixed" impedance transformer (also referred to as 2nd stage matching and made of stub and trombone tuners) transforms the low Z_{CT} value (possibly including a small reactive part) to Z_0.

The ILA project started in 2001 with the aim of demonstrating :

- Coupling of ICRF power to plasmas in conditions relevant to ITER.
- Achieving a power density in the range of 8-10MW/m^2.
- Reliable operation at 45kV on an ELMy H-mode plasma.
- Passive matching tolerant against load perturbations caused by ELMs.

The what follows the experience gained with the ILA on testbed and on JET plasmas is described. A summary of the results obtained and lessons learned for the design and operation of the ITER ICRF system is presented in Table 1.

2.1 ILA DESIGN AND COMMISSIONING ON TEST BED

The ILA for JET was designed to be capable of coupling 7.2MW across the frequency range 30-55MHz using a close-packed array of straps, with ELM tolerance incorporated using an internal conjugate-T junction. The 8 short low inductance straps are mounted as four RDL's arranged in a 2 toroidal by 2 poloidal array (Fig.1a). Each RDL consists of two poloidally adjacent straps which are fed through matching capacitors located in-vessel from a T-junction which in turn is fed from a 1.76m long vacuum transmission line with a characteristic impedance of 9Ω which, as part of the 2^{nd} stage matching circuit, transforms a Z_{CT} of 3Ω into 30 Ω at the mid-band frequency of 47.5MHz (Fig.1c). The accessible coupling was determined by the following constraints (see Fig.3):

- The capacitor range, 80–300pF, mainly delimiting the lower and upper frequency bounds : the limits shown are for single independently powered RDLs. When the mutual coupling between the straps of the antenna array cannot be neglected, the bandwidth of the system can be modified. The amount of modification is not trivial due to nature of the matching problem: for N coupled RDLs the 2N independent quadratic equations for the values of the matching components in absence of mutual coupling become a set of 2N simultaneous polynomial equations of order 2N which exhibit a much more complex solution space [10].
- The current through the matching capacitor, Ic, delimits the maximum pulse length (scaling inversely with I^2_c), which is specified to be 10s for 1250Arms at 55MHz. Depending on the

coupling and/or the frequency the pulse length could be longer or the maximum capacitor current at 30MHz could be higher, up to 1480Arms. This should allow a pulse length of 10s for currents up to 1250Arms at mid-band frequency (equivalent to a coupling of 2W/m).

- The strap feeder and capacitor voltages, respectively, VF and VC, delimit the lowest coupling reachable for a given voltage stand-off.

During the design phase of the ILA, tests on a high power prototype (HPP, ORNL and PPPL, USA) confirmed its overall RF functional design on a single RDL [11, 12]. 3D RF modelling using CST-MWS [13] was validated by measurements of the two-port HPP antenna strap scattering matrix and a voltage stand-off of 45kV for short pulses (50ms) was demonstrated. For longer pulses issues related to the RF losses in the antenna straps and antenna box side walls became apparent. These RF losses led to partial melting of the antenna housing side walls as well as the strap edges where the RF current density is the highest. Recommendations and actions for the final design of the ILA resulting from these tests were incorporated into the design of the various components in time for the start of their manufacturing phases. The main components thus improved were the antenna strap edges, antenna box side walls and the distance between the antenna private limiters and the antenna housing.

Once manufactured and its components delivered to the JET site, the antenna array scattering matrix was measured using a salted water tank to simulate a plasma load [14, 15] and various RF signals, the Antenna Pressurised Transmission Line (APTL) forward and reflected directional couplers for each RDL and the voltages probes, two for each capacitor, were calibrated. The latter calibration can only be done when the antenna is not mounted on the Vacuum Transmission Line (VTL) Outer Support Box and is rather complex, involving parameter fitting of an RF model to the measured data [16]. After the high power test and commissioning phase on test bed described hereafter, we found that the initial calibration was overestimating the voltages by about 7%. The calibration factors were corrected for the operation on plasma but the consequence was that the voltages achieved on test bed were 42kV rather than the target 45kV. Although there were no signs that this voltage was a hard limit it was decided to limit the maximum voltages during the commissioning phase on plasma to the voltages really achieved on test bed.

Subsequently, the ILA was fully assembled on the JET RF testbed facility and the 4 RDLs were matched separately in turn at low power at 42MHz on vacuum and tested at high power.

The various conditioning phases, multipacting, increasing pulse lengths at moderated power, short pulse voltage hardening and finally going to long pulse high voltage, were carried out without major issues aside from one capacitor failing due to an uncontrolled RF power surge. About 250kW per RDL was required to reach 42kV corresponding to a dissipation of 1MJ per RDL [17, 18].

The multipactor conditioning phase required only 50 to 100 pulses for each of the 4 RDLs. This was followed by an outgassing conditioning phase at medium voltage and modest power (10-50kW) of about 250 multi-second pulses. The short pulse high voltage conditioning phase was very smooth and 42kV / 100ms were reached in about 250 pulses (average power kept below 1.5kW). The power

needed to reach maximum voltages was about 250-280kW giving an efficiency of about 88% at the expected plasma coupling. Although this power is less than the High Power Prototype [19] due to the additional Cu plating on the straps and Ni plating of the antenna housing, it is slightly higher than the 200kW expected. During conditioning one capacitor of the Lower Left RDL (straps 3 and 4) was damaged due to a generator control issue : the capacitor was replaced and this RDL was re-commissioned. For the Upper Right RDL (straps 5 and 6), the first one tested, a mismatched transmission line between the testbed and the RF generator building made long pulse operation difficult. For the other RDLs tested, long pulses (~100) were used dissipating about a third of the energy corresponding to 10s long full power pulses on plasma. Due to technical difficulties with the recording of the IR camera data, increasing the dissipated energy further towards its nominal value was not attempted. The observed temperature increase on the Ni-plated side walls of the antenna housing of the bottom strap ranged between 105 and 150 °C/MJ (assumed emissivity of 0.15).

Another important aspect of the commissioning on testbed was the testing of algorithms for simultaneously matching all 4 RDLs making up the ILA.

The ZCT matching algorithm [20] was implemented on a control PC running Labview [21] and successfully used to home in on a match of the 4 RDLs simultaneously at different frequencies and for various toroidal antenna phasings (29MHz (dipole), 33MHz (dipole), 42MHz (monopole, dipole)) as well as different target $Z_{CT} = R_{CT}$ (3 and 6Ω) + jX_{CT} (ranging from −2 to +2Ω). At the higher frequencies, the matching succeeded for either the lower or upper half of the ILA separately (47MHz (dipole, using the algorithm), 49 MHz (dipole, manually adjusted)). Matching at 51MHz appeared only possible manually for single RDL's.

The rather severe upper frequency band deficiency, effectively reducing the ILA upper frequency to 47MHz at best, was analysed in 2008. A 3D electromagnetic analysis was done of the whole circuit comprising straps, capacitors including their internal build-up and the T-junction. Such analysis had not been possible in a timely manner and with the means at hand during the ILA design phase in 2001-2002. This modelling identified clearly the main cause of the deficiency : the capacitor cannot be considered as a lumped element (including its series inductance) located between the antenna strap feeder flange and the "bridge" (the region of connection between the two branches of the RDL circuit) (Fig.4). Indeed it appears that the internal part of the capacitor that houses the flexible bellows allowing to move the capacitor's variable electrode, causes an effective electrical length to be added to the strapcapacitor branch. This results in marked lower resonance frequencies for given capacitor settings. The problem is further compounded by the relatively high crosscoupling between the 4 RDLs making up the ILA [10]. Resolving this issue requires to redesign the capacitor in order to remove the bellows section from the RF path by e.g. using sliding contacts inside the capacitor's private vacuum. This is by no means straightforward when considering the capacitor's various manufacturing and assembly steps and its thermal and chemical conditioning. It would certainly have been a rather large departure from the projects initial assumption that the capacitors required only modest modifications to be fit for their use on the ILA and would not have fitted the

project's budget and time scopes.

It was observed that the setting of the various 2nd stage and main phase shifters is rather critical to obtain a correct voltage distribution on the 8 ILA straps and to make the matching algorithm converge to and remain in a stable solution. This is due to the rather large cross-coupling between adjacent toroidal straps as well as the 4 inner straps (2,3) and (6,7) (Fig.1a, 1b) : slight voltage phase differences away from 0 or π cause a power transfer between RDLs which can be further enhanced by the capacitors adjusting (asymmetrically) to the modified matching solution. This behaviour was also observed on numerical simulations of the matching algorithm as well as during the plasma commissioning phase and is discussed in detail in section 2.2.3 hereafter.

2.2 OPERATIONAL EXPERIENCE OBTAINED WITH THE ILA

2.2.1 Delivering ICRF power on L- and H-Mode Plasmas

Following its commissioning on testbed [22], the ILA was installed on JET in 2007 and commissioned on plasma from May 2008 to March 2009. During this period, successful operation of the ILA on L- and H-mode plasmas was achieved at frequencies of 33 and 42MHz (with a few pulses at 47 MHz) [17, 23]. Up to 4.76MW of ICRF power was coupled to L-mode plasmas (Pulse No: 75329) and power densities up to 6.2MW/m^2 (JET Pulse No: 73941 see Fig.5) were reached (2.80MW from the antenna lower half for a total ILA Faraday Screen surface ~0.91m^2). This value is in the range of what is needed for the ITER ICRF system: 6 to 8 MW/m^2.

On H-mode, the maximum coupled power was less than expected due a lower antenna loading than was assumed during the design of the ILA. A maximum coupled power of 1.88MW was achieved (JET Pulse No: 78070) from the ILA upper half corresponding to a power density of 4.1MW/m^2 (Fig.6). The simultaneous operation of the ILA upper and lower half on H-mode plasmas (see section 2.2.3) as well as RF power plant issues slowed down progress to achieving higher power or power densities before a capacitor failure curtailed ILA's operation (see section 2.2.5).

2.2.2 Voltage Stand Off

The ability to operate an ICRF antenna reliably at voltages above 40kV is a critical aspect for the future ITER ICRF antenna. Indeed, a fundamental limitation of the A2 antenna system is its unfavourable ratio of average strap current, the square of which determines the power coupled, to the maximum system voltage, further compounded with limitations on the latter. These issues were addressed during the design of the ILA : this ratio was improved by a factor between 1.5 and 2 and the system voltage was raised from 35kV achievable on the A2 antenna system to a target of 45kV. Operation at maximum voltage of 42kV (Fig.7) was achieved easily and reproducibly on L- and H-mode. Note that the maximum voltage was restricted by the decision not to exceed the voltages achieved on testbed (see the calibration issues mentioned earlier). The maximum electric field of the antenna structure in torus vacuum is located on the matching capacitor's corona ring connected to the strap's feeder and is 2.5kV/mm at 42kV in all directions with respect to the total magnetic

field. Inspection of the extracted vacuum transmission lines carrying the matching capacitors did not reveal obvious traces of arcing or other damage in this area. A statistical analysis of all the ILA data shows that about 18% of the 1603 ILA pulses recorded on the ILA control computer (excluding pulses predating this recording and concerning the first low level ILA commissioning) fail due to causes not related to the antenna itself (test pulses for commissioning the arc detection, JET pulses disrupting before the RF pulse, RF plant issues, hydraulic plant and capacitor control issues, …). Figure 8 shows that the quality factor, Q, calculated for the remaining 1309 pulses, and defined as the ratio of the delivered to the requested energy when the former has reached 97% of its total, does not degrade with increasing voltage and power.

2.2.3 Matching

The conjugate-T feeding circuit demonstrated tolerance to the load variation occurring during ELMs (see Figs. 6 a, b, c). By setting appropriate values of the impedance at the T-junction, Z_T, $Re(Z_T)\sim 3\Omega$ maximizes the load resilience properties while $Im(Z_T)\sim -2\Omega$ balances the voltages on the straps fed from the T-junction), and at the 2nd stage impedance transformer, it was possible to keep the VSWR on the amplifier output transmission line below the level (VSWR = 2.7) at which the transmitter is tripped for safety. Nevertheless, the simultaneous operation of the whole antenna, particularly in H-mode, posed difficulties due to the cross-coupling between the individual straps. While full array operation is relatively easy to achieve on L-mode plasmas due to higher and quiescent loading, such operation in H-mode required a tight control of the phasing of the various straps with respect to each other (to minimise the cross-coupled power) as well as a careful setting of the impedances of the 4 T-junctions (to optimise the load resilience) and post pulse analysis software had to be used to converge on a shot by shot basis to the optimal settings for the impedance transformers. A successful example is represented on Fig. 9 where steady power is maintained during the L to H mode transitions. Unfortunately one of the capacitors developed a leak shortly after so that further development to higher power and performance of this operation was not possible. In what follows more details are presented on the matching aspects of the ILA.

2.2.3.a Control of the ILA antenna system

The ILA is controlled by several feedback systems [15] as shown in Fig.10: (i) the 4 complex T-point impedances Z_{Tkl} ((kl) = (12), (34), (56), (78); k and l refer to the strap numbers (Fig 1b)) are feedback controlled using the variable capacitors C_k,C_l with the imaginary part of Z_{Tkl} set (iteratively on a shot to shot basis) to achieve equal voltage amplitudes on the capacitors/straps $|V_k/V_l| = 1$ within each RDL; (ii) the phase shifter and stub lengths lk,ll ("second stage" elements) are manually adjusted to achieve an "offset" match in order to avoid exceeding the VSWR limit during (large) ELM excursions; (iii) the relative phasing of the generators is adjusted using a real-time feedback control to achieve a tight phase control of the feeder voltages of the straps with the highest cross-coupling (2, 3, 6, 7). The experimental accuracies on the settings are ±0.1pF on the

capacitor values (±20μm actuator position), ±5cm on trombone and stub lengths and ±5° on the imposed generator phasing.

2.2.3.b Setting the second stage "OFFSET" match

Figure 11a shows the time evolution during L- and H-Mode of the D_α intensity, Z_T and VSWR measured in the Main Transmission Line (MTL) between the generators and the second stage matching circuit. Fig. 11b shows the measured T-point impedance Z_T in the complex plane during L- and H-mode, together with circles of constant Voltage Standing Wave Ratio (VSWR) = 2.0 for two sets of lengths ls, lt. If the second stage is set to match Z_T during L-mode or H-mode between ELMs, the VSWR limit will be exceeded with the ELM excursions. A retraction of the stub by 15cm targets the average Z_T reached during the ELM excursions and avoids exceeding the generator VSWR limit.

2.2.3.c Feedback control for the inner strap phase

Operation of the ILA on testbed and plasma showed that the forward voltage phases on the feed lines could not be set to fixed values and prevented the capacitor voltages to evolve with respect to each other as can be seen in Fig. 12a. Although the Z_{Tkl} remain constant, small phasing errors lead to power transfers between RDLs that causes the capacitors Ck and their voltages V_k to drift in time. Simulations show that the drift is the start of a general evolution towards a steady state solution with fixed Z_{Tkl} but asymmetrical voltages V_k. To operate the antenna stably and within safe voltage limits, the 3dB combiners and splitters (see Fig.2 of [24]) were removed and the existing JET RF plant generator phase control systems [25] were re-used to feedback control the 4 inner strap voltage phases ($\psi 2, \psi 3, \psi 6, \psi 7$) (in principle the implementation of a feedback control loop on the trombones adjusting the phasing between the 4 RDL would also have been possible, however it would have taken more time than to simply bypass the 3dB combiner-splitter couplers and use the existing RF source phase controls). Initially, the relative generator phases $\phi 34$, $\phi 56$, $\phi 78$ were set such that the inner strap voltage phase differences are $\psi 3 - \psi 2 \approx \psi 6 - \psi 2 \approx \psi 7 - \psi 3 \approx \pi$. The improvement with this modification can be seen in Fig. 12b. As a downside of these modifications, problems were often experienced running the full antenna array with 4 interacting generators. Generators not all starting simultaneously and/or the appearance of oscillations of growing amplitude during power ramp up (suspected to be related to the phase feedback control) caused excessive tripping and termination of these full array pulses.

2.2.3.d Adjusting the relative phase between the generators

With the antenna facing a salty water load [14, 15] closely fitting the Faraday screen curvature, full antenna strap array impedance matrix and scattering parameter measurements could be done. With the antenna operating on plasma, such complete measurements were no longer possible. An effective resistive loading R_{Ckl} per RDL at the position of the capacitor voltage RF pickup probes

can still be calculated as shown in Fig.13. For the measurements on a salty water load, similar values of Rckl per RDL were obtained, while for measurements on plasma with the relative generator phasing initially set such that $\psi 3-\psi 2 \approx \psi 6-\psi 2 \approx \psi 7-\psi 3 \approx \pi$, the effective loading of the upper half of the antenna was higher than for the lower half (see Fig.14, 11–14s).

This difference is caused by the triangularity of the plasma putting the plasma separatrix on average ~3cm further away from straps of the lower RDLs as compared to the upper ones. To achieve maximum power transfer and optimal ELM resilience, all voltages over the antenna strap array should be made equal in amplitude. This can be done by using the reactive mutual coupling with the proper imposed phasing of the generators to create a power transfer between the upper and lower RDLs, as demonstrated during JET Pulse No. 75173 in Fig.14. The initial settings for the relative inner strap phasing for the start of the pulse from 11–14s was obtained experimentally to equalize the effective resistive loading within the upper half RC12 = RC56 and RC34 = RC78 within the lower half of the ILA separately. From 14/16/18s, the inner strap up/down phasing $\psi 3-\psi 2 \approx \psi 7-\psi 6 \approx \pi+$ is varied by sweeping from 0°/+15°/–15° from these initial values and one sees the corresponding change in effective load resistance and capacitor voltage until they are all equalized near the end of the pulse with = –15° .

2.2.3.e Possible future improvements to the ILA matching and feeding circuit

Considering the experience gained and in order to improve the use of the ILA in case it gets repaired and used in future experimental programs at JET, it is necessary to propose following modifications / additions to the layout and control of the matching and feeding circuit :

i) Although the matching algorithm for setting the capacitors worked reliably and satisfactorily, the correct set up of the second stage matching circuit to maximize the load resilience was rather tedious and required several JET pulses. As this set up is depending to some extent on the experimental conditions (base load and load excursions due to ELMs vs, the optimal offset match for the 2nd stage), a major improvement should be to control the 2nd stage in a feedback control loop together with the capacitor matching algorithm.

ii) The removal of the 3dB coupler combiner-splitters from the feeding circuit led to technical issues related to the simultaneous start of the 4 RF sources feeding the ILA. Even if not effective for the matching of the ILA, the reinsertion of the 3dB hybrid coupler / splitters in the feeding transmission line circuit will provide a kind of RF insulation between the 4 RF sources thereby substantially improving the conditions at the start of the RF pulse and decrease the number of failed pulses due to these issues.

2.2.4 ARC DETECTION

Successful implementation of ELM-tolerant matching revealed a new challenge to high-power ICRF operations in H-mode plasmas. Together with previously observed antenna breakdowns at high voltages, occurrences of ELM-triggered arcs have been observed on both the External Conjugate-T

(ECT) and 3dB systems installed on the A2 ICRF antennas on JET despite a substantial reduction of the voltages in conditions of high antenna loading occurring during ELMs [1]. Both simulations [20] and measurements [9] have shown that the traditional arc detection method based on monitoring the VSWR in the matched transmission lines is inadequate for antenna protection. To cope with this difficulty on the ILA, a novel arc detection method based on a redundancy check of the real-time measured voltages on the antenna straps and the currents near the T-junction was developed. Since this scheme requires the knowledge of the 3-port scattering matrix it was named Scattering Matrix Arc Detection (SMAD). The principle of operation is simple: for each RDL, the forward power (before the T junction) and the strap voltages are used in conjunction with the scattering matrix and the matching capacitor values to compute the reflected power, which can be directly compared to the measured reflected power to produce an error signal. If the error signal (in its simplest form the difference between the measured and computed reflected power values) is above a user imposed limit value for more than a certain (user imposed) time window, the SMAD system sends a trip signal to the generator to shut-down the RF power. The cycle time of the SMAD system is 2ms. For the generator power interruption to occur a number (user imposed) of consecutive SMAD arc detections are required, typically about 5; an arc is thus positively detected after about 10ms depending on the exact settings, while the shut down time of the RF generators is about 40-50ms. In practice it was noticed that finetuning of the SMAD coefficients (originally computed via modelling of the antenna 3- port junctions) was necessary for each operating frequency to adjust the error signal to its minimum level. Once these 'calibration steps' were overcome, the SMAD system has shown to be very robust to false positives and nevertheless very sensitive to even small arcs occurring inside the detection region. A detailed description of the SMAD system and several examples of arcs detected in different regions of the ILA system is given in [26]. It is important to stress that, by definition, SMAD only covers a restricted part of the antenna circuit (the region between the strap voltage measurements and the forward / reflected power measurements) and the additional use of other arc detection systems (such as VSWR) is still necessary to protect the higher impedance regions of the RF system as e.g. the transmission lines.

In parallel, a second arc detection system was implemented on JET, the so-called Sub-Harmonic Arc Detection (SHAD) which looks for characteristic frequencies below the operating frequency of the RF system, emitted by arcs [27]. The SHAD detection band on JET is 5-20MHz, and the system has shown its principal capability to detect arcs on JET [28]. However, it was also found to be sensitive to parasitic signals in this frequency band [29], from other sources, like e.g. Ion Cyclotron Emission in the plasma, voltage breakdown events in the Neutral Beam Injection system, etc. and further developments are required to obtain a reliable system. Similar effects have been seen on ASDEX-Upgrade [30, 31].

2.2.5 The ILA capacitor failure.

After less than one year of operation, sudden difficulties to match the lower half of the ILA (JET

Pulse No: 77743) were traced to the failure of one of the capacitors. Subsequent analysis and a dedicated test on a spare capacitor put the development of a micro-leak of the capacitor's bellows leading to a degradation of the capacitor's private vacuum as the most plausible cause. All eight ILA capacitors had undergone an estimated 3000 cycles before this failure, in a combination of operation on the test bed and during operations on JET. During the design and construction phase of the ILA, specific R&D on the bellows' lifetime was carried out showing a lifetime ranging from 18000 to 35000 full stroke cycles qualifying them for use on JET : two years of full time operation were estimated to require 5000 cycles. Furthermore, in practice, the required capacitor movements seldom necessitate more than half stroke cycles or even less.

The discrepancy between the pre-manufacture bellow tests and the real operation of the bellows might possibly be due to the fact that during the tests, for the sake of simplicity and total cost of the tests, the bellows were set up pressurised with air with respect to the surrounding atmospheric pressure and the failure observed as a loss of bellows internal air pressure. It is possible that micro-leaks appeared well before a measurable macroscopic decrease of the pressure. Such minute leaks however rapidly degrade the capacitor's sealed private vacuum and ruin its voltage stand off.

2.3 IMPURITY RELEASE STUDIES

An important question about operation at high power density was whether or not it would increase the impurity influx into the plasma due to RF sheath effects. Figure 15 shows that the impurity influx from the ILA is in fact slightly lower than for the A2 antennas for comparable total power coupled [32] knowing that the ILA data pertains to 5 to 10 times higher power densities than that of the A2 antennas. Although there are objective differences between the A2's and the ILA's front face designs as well as electrical grounding to adjacent protective limiter structures that explain this result, it proves that high power density antennas can be designed that do not imply a high impurity influx [33].

2.4 COUPLING STUDIES

Dedicated pulses were performed where the distance of plasma separatrix to the ILA straps was varied while measuring all relevant plasma density and temperature profiles. The power coupled to the plasma can be expressed in terms of the RF quantity "effective conductance" Geff (measured at the RF probe fixed capacitor flange position) and defined as:

$$G_{eff} = \frac{2\mathrm{Re}(P^{+}_{couplers})}{V_{capacitor1} + V_{capacitor2}}$$

with $P^{+}_{couplers}$ the power measured at a directional coupler just before the T-junction and $V_{capacitor1}$ and $V_{capacitor2}$ the voltages at each of the capacitors of the RDL. The good agreement between the modelled and measured Geff values is illustrated on Figure 16 for a JET L-mode plasma where the estimated error bars are also shown. The horizontal bars pertain to the uncertainties on the exact

position of the separatrix (±1cm) while the vertical error bars pertain to the uncertainties on the RF voltage and power measurements (±21%). Initially, this low measured ILA coupling on JET (Lmode 1.5Ω/m, H-mode ~0.8Ω/m) compared to original design values (L-mode ~2.0 and H-mode ~4Ω/m [6], estimates made without availability of TOPICA [35, 36] at that time), raised concerns about achieving the TOPICA [37] and ANTITER [38] predicted 20MW coupled power per antenna on ITER H-mode plasmas, especially given the higher first wall to plasma seperatrix spacing. However, a qualitative comparison of JET and ITER RF coupling physics considering antenna geometry and plasma profiles [39] shows the lower than originally envisaged coupled powers on JET not to be inconsistent with the more favourable ITER coupling predictions. The above results together with previous results from Tore Supra [40], DIII-D [36] and Alcator-C [35] validate the use of TOPICA to predict the performance of the ITER ICRF antenna.

Recent more detailed studies show [41] that under the condition of sufficient single pass absorption in the bulk plasma, the coupling to an inhomogeneous edge plasma is determined by (i) the distance between the antenna and the location x_{CO} of the cut-off density NCO corresponding to most excited $k_{||}$ value in the antenna $k_{||}$ power spectrum; (ii) the distance between x_{CO} and the location xmax of a density N_{max}, equal to several times the cut-off density, and (iii) the density gradient between this N_{max} value and the bulk density N_{bulk} (Fig.17). This divides the zone between the antenna and the bulk plasma in three regions, and reflects the following underlying physics : for region 1 +2: optimization of wave coupling through an evanescent zone and for region 3: minimization of wave reflection. A detailed analysis shows that small modifications in the profile can strongly improve the coupling properties, and this should leave margin for adapting the profiles, provided that the measures taken have a minimal influence on the energy confinement of the plasma. E.g. gas puffing could be used to produce a density a few times larger than the cut-off density NCO as close as possible to the antenna, or one could avoid a too steep density gradient up to the bulk plasma to reduce wave reflection. This is a subject of ongoing experimental work on several tokamaks, including Tore Supra, ASDEX and JET, and falls out of the scope of this paper [42].

3. EXPERIENCE GAINED FOR THE DESIGN AND OPERATION OF AN ITER ICRH SYSTEM

ICRF Issue	JET ILA Result	Implications for ITER **positive conclusion are in bold;** warnings are underlined;
Modelling	The measured coupling agrees within error bars with that predicted using TOPICA.	**Within the limits imposed by measurement errors, the JET results validate the TOPICA code on L-mode plasma**.
Coupling.	The JET ILA coupled a maximum power of 4.76MW at 30kV in L-mode with 4cm ROG (separatrix to first wall spacing) at 42MHz (shot 75329), corresponding to coupling of order 2.1Ω/m. More generally, coupling of the order of 1.5Ω/m was obtained for a wide variety of L-mode plasmas at 4cm ROG. This dropped to a maximum of approximately 0.8Ω/m in H-mode at 5cm ROG.	**The coupling achieved in L-mode is consistent (within error bars) with that predicted by TOPICA for ITER H-mode,** providing that the ITER density profiles provided by the ITER Organization can be achieved. Since the ITER coupling specification has been derived using TOPICA, the key conclusion is that **the low coupling achieved in JET H-mode using the ILA does not contradict the higher coupling presently computed for the ITER ICRF antenna.**
Operation at high RF voltage	Voltages of up to 42 kV have been achieved on a semi-routine basis on both test-bed and JET (the operations team decided to use a 42kV limit, rather than the design point of 45kV to provide margin for safe performance in this first phase of the use of the ILA).	The ease with which the JET ILA achieved operating voltages of 42kV suggests that **the decision to base the ITER antenna on a 45kV looks sound, from the perspective of arcing close to the antenna straps.** The in-vessel matching system used on the ILA means that the voltages present on the antenna behind the vacuum capacitors are substantially lower than the target 45kV and so the ILA has not validated the ITER voltage/electric field levels on components within the rear section of the antenna and the pressurised transmission lines .
ELM tolerance	A limited number of shots were possible at the target 3Ω T-point impedance, due to plant availability issues as well as the late commissioning of the arc detection system. Nevertheless, ELM tolerance was successfully demonstrated for a wide range of plasma conditions. As expected, for cases with very low baseline coupling and very high load change during ELMs, the VSWR could not be maintained below the trip levels.	**The results from the JET ILA (and the JET external conjugate-T system) have confirmed the feasibility of using a conjugate-T system to achieve ELM tolerance in large ELMs**
Matching	Simultaneous matching of the 4 RDLs was achieved. Problems were encountered, and only partially overcome, as follows: 1. Tripping caused by slight differences in turn-on time between the four RF amplifiers combined with the level of cross-coupling between RDLs. 2. The load resilience can become insufficient at low coupling, i.e. it is not possible to keep VSWR < 1.5 (2) before, during and after the ELM (see also ELM tolerance). 3. The detailed adjustment of the several RDLs with respect to each other was difficult to obtain with sufficient precision which leads to a degradation of the load resilience.	If a conjugate-T system is to be adopted on ITER (the back-up option): 1) **The proposal to match four systems on ITER, appears to be sound [43]** 2) The effect of cross-coupled power on the simultaneous operation of all amplifiers should be assessed and possibly mitigated (e.g. using decouplers [44]). 3) Based on the coupling predictions for ITER, **it is not expected that limitations in ELM tolerance due to low coupling should be an issue**. (see also ref. 43)
Coupled Power density	The antenna coupled power densities of up to 5.7MW/m^2 L-mode (JPN 73941) and 4.1MW/m^2 H-mode (JPN 78070).	The JET ILA has confirmed that operation at power densities up to 4-5MW/m^2 is feasible without excessive arcing, and only failed to test the target 8MW/m^2 due plant problems outside of the antenna. **The use of close-packed short straps to achieve such power densities did not pose any unforeseen problems.**
Impurity Generation	On-going analysis have shown that with increasing the ILA power a small increase in Ni (up to ~ 10^{-2} %), Chromium and Iron (up to ~ 0.3 10^{-2} %) is observed. It is interesting to note that the operation of an A2 antenna produces similar (or slightly higher) level of Nickel, Chromium and Iron leading to the conclusion that there is no adverse effect linked to the ILA higher power. Note that no Beryllium or Carbon increase was observed.	**No direct link between high power density and high impurities content was observed.** The main candidate for the observed small level of impurities are the RF sheaths effects that might lead to ions sputtering. Any high Z impurities should de avoided in the front face or limiter surrounding the ICRF antennas.

ICRF Issue	JET ILA Result	Implications for ITER **positive conclusion are in bold;** warnings are underlined;
Heating Efficiency	The results obtained are very similar to the A2 antennas when used in similar conditions. Typically 4 MW of ILA power used for central H minority heating will lead to a central electron temperature of ~ 6 -7 keV, with fast ion energy content ~ 2 to 3 MJ depending of the H concentration. Note that the presence of high energy H tail was confirmed by the gamma-ray diagnostics and was found to lead to strong sawteeth stabilisation as expected for plasmas with the H resonance cyclotron layer placed into the q=1 surface .	**There is no evidence that high power density could led to extra power losses in the SOL.**
Arc detection	The following arc detection systems have been used: standard VSWR and Scattering matrix (SMAD) systems. The existing VSWR system worked in its standard mode, but with expected limitations of failure to trip in anticipated circumstances (close to the T-point). The SMAD system designed to allow safe operation at low conjugate-T impedance (3Ω) used for ELM tolerance, was implemented and arcs successfully detected. Sub-Harmonic arc detection (SHAD) has been tested. The ability of the SHAD to detect arc in L-mode and H-mode was confirmed and its connection to the plant trip system is envisaged although in H-mode, the adjustment of the signal differentiating noise / trip level still need further optimisation.	**A new arc detection system (SMAD) has been successfully commissioned on JET**. <u>The complexity and reliability of all present arc detection systems, however, is such that further arc detection schemes would be highly advisable in order to avoid problems with false positives, and, in particular, false negatives.</u>

Table 1 : Summary of the results obtained during the ILA commissioning and experience gained for the design and operation of an ITER ICRF system.

CONCLUSIONS

The ILA was successfully assembled and tested on testbed. The matching studies on test bed allowed testing of the matching algorithm in conditions easier than would have been the case on JET plasmas. The most severe deficiency observed was the shortfall of the frequency bandwidth which limited the operation of the ILA to about 49 MHz at best instead of originally specified 55MHz.

The ILA was subsequently installed and commissioned on JET. Its operation on a range of plasma configurations and antenna frequencies led to key ITER-relevant results :

1. The ITER-relevant use of a high power density conjugate-T configuration was confirmed. ELM tolerance was obtained with a conjugate-T configuration operating at low real impedance at the conjugate-T point. The ILA demonstrated operation at 42kV and electric fields of 2.5kV/mm regardless of their orientation with respect to the magnetic field on JET in L- as well as H-mode without observable degradation of the pulse quality inherent to voltage handling capabilities. This antenna has demonstrated efficient trip-free ELM tolerant operation with power densities up to 6.2MW/m^2 on Lmode and 4.1MW/m_2 in H-Mode, which is substantially higher than was previously possible in JET.
2. Control of the antenna matching elements in the presence of high mutual coupling between straps using four conjugate-T systems proved feasible (but did require several developments of the matching system). The matching on ELMs sometimes suffered from the low coupling in H-mode, but it was in general possible for operation on pairs of RDLs to keep the VSWR excursions between 2 and 2.5 by properly offsetting the 2nd stage match.

3. Antenna arcing during ELMs has been identified as an emerging challenge for load-tolerant ICRF systems. Validation of arc detection systems on conjugate-T configurations in ELMy H-mode plasmas [18, 21]. The Scattering Matrix system (SMAD) operated successfully and the Sub-Harmonic system (SHAD) proved to be efficient, although the system was found sensitive to parasitic signals.
4. No detrimental effects on impurity generation or loss of heating efficiency from operations at high power densities as demonstrated on the ILA
5. Successful validation of the TOPICA coupling code allowing to favourably extrapolate the feasibility of the 20MW ICRF system planned for ITER.

The ILA, together with the External Conjugate T and the 3dB system implemented on the JET A2 antenna systems, demonstrated that the use of load tolerant systems allowed to couple high levels (> 8MW) of trip-free ICRH power injection into ELMy and Advanced Mode plasmas and considerably expands JET's research capabilities [0].

ACKNOWLEDGEMENTS

This work, supported by the European Communities under the contract of Association between EURATOM and CCFE, was carried out within the framework of the European Fusion Development Agreement. The views and opinions expressed herein do not necessarily reflect those of the European Commission. This work was also part-funded by the RCUK Energy Programme under grant EP/G003955.

REFERENCES

[1]. M. Graham et al., this edition.
[2]. F. Durodié et al., 14th Top. Conf. on RF Power in Plasmas, AIP Conf. Proc. 595 (2001) 122
[3]. M. Vrancken et al., SOFT 2010, Performance of the Scattering Matrix Arc Detection System on the JET ITERlike ICRF antenna
[4]. T. Wade, private communication / JET internal memo 1998
[5]. G. Bosia, High-power density ion cyclotron antennas for next step applications, Fusion Science and Technology **43** (2003) 153–160.
[6]. ITER Detailed Design Description, Ion Cyclotron Heating and Current Drive System, WBS 5.1 (1998); https://user.iter.org/?uid=29KRRG
[7]. D. Hoffman et al., 7th APS Topical Conference on Applications of Radio-Frequency Power to Plasmas, AIP Conf. Proc 159 (1987).
[8]. I. Monakhov, et al., Fusion Engineering and Design **74**, 467-471 (2005)
[9]. I. Monakhov, et al., 18th Topical Conf. on RF power in Plasmas, AIP Conf. Proc.1187, (2009) 205
[10]. P.U. Lamalle, Fusion Engineering and Design **74** (2005) 359
[11]. R.H. Goulding et al., 15th Top. Conf. on RF power in Plasmas, AIP Conf. Proc. 694 (2003) 102

[12]. R.H. Goulding et al., 20th IAEA Fusion Conference, Villamoura, paper FT /1-3 (2004)
[13]. CST MICROWAVE STUDIO®, User Manual Version 2009, Sep. 2008, CST AG, Darmstadt, Germany, www.cst.com.
[14]. A.Messiaen et al, Fusion Engineering and Design **74** (2005) 367
[15]. M.Vrancken et al, Proc. 17th Top. Conf on RF power in Plasmas, AIP Conf. Proc. 933 (2007) 135.
[16]. M. Vrancken et al., Fusion Engineering and Design, **82** (2007) 873-880.
[17]. F. Durodié, et al., 18th Topical Conf. on RF power in Plasmas, AIP Conf. Proc.1187 (2009) 221
[18]. M. Nightingale et al., 22th IAEA Fusion Conference, Geneva, (2008) paper FT/4-5Ra
[19]. R.H. Goulding et al., 16th Top. Conf. on RF power in Plasmas, AIP Conf. Proc. 787, (2005) 194
[20]. M. Vrancken et al., 18th Top. Conf. on RF power in Plasmas, AIP Conf. Proc.1187 (2009) 225
[21]. Labview, National Instruments, www.ni.com/labview
[22]. F. Durodié et al., 17th Topical Conf. on RF power in Plasmas, AIP Conf. Proc. 933, (2007) 131
[23]. F. Durodié, et al. , Fusion Engineering and Design, Volume **84** (2009) 279
[24]. F. Durodié et al., Fusion Engineering and Design **74** (2005) 223
[25]. A. Kaye et al., Fusion Technology **11** (1987) 203
[26]. M. Vrancken ,et al., 18th Top. Conf. on RF power in Plasmas, AIP Conf. Proc. 1187 (2009) 237
[27]. F. Braun and Th. Sperger. "An Arc detection system for ICRF heating", in Proc. of 19th Symposium on Fusion Technology, Lisbon, (1996) 601
[28]. P. Jacquet et al., 18th Top. Conf. on RF power in Plasmas, AIP Conf. Proc. 1187 (2009) 241
[29]. P. Jacquet et al, 19th Top. Conf. on RF power in Plasmas, paper B-22, AIP Conf. Proc., in print.
[30]. R. D'Inca et al., 17th Top. Conf. on RF power in Plasmas, AlP Conf Proc. 933 (2007) 203
[31]. R. D'Inca et al., 19th Top. Conf. on RF power in Plasmas, paper R-02, AIP Conf. Proc, in print
[32]. A. Czarnecka ,et al., Proc. 36th EPS Fusion Conference, paper P-2.146, (2009)
[33]. V. Bobkov, et al., 18th Topical Conf. on RF power in Plasmas, AIP Conf. Proc.1187, (2009) 125
[35]. V. Lancellotti et al., Nuclear Fusion **46** (2006) S476
[36]. R. Maggiora et al., Nuclear Fusion **44** (2004) 846-868
[37]. D. Milanesio, et al. 18th Top. Conf. on RF power in Plasmas, AIP Conf. Proc.1187 (2009) 233
[38]. A.Messiaen et al, Nuclear Fusion **50** (2010) 025026
[39]. M.P.S. Nightingale, et al., 18th Top. Conf. on RF power in Plasmas, AIP Conf. Proc.1187 (2009) 213
[40]. D. Milanesio et al., Plasma Physics and Controlled Fusion **49** (2007) 405-419
[41]. A.Messiaen et al, Nuclear Fusion **53** (2011), 085020
[42]. M.-L. Mayoral, et al. 23rd IAEA Fusion Conference, Daejon, Paper ITR/P1-11
[43]. D.Grine et al., 18th Top. Conf. on RF power in Plasmas, AIP Conf. Proc.1187, (2009) 285
[44]. A.Messiaen et al., Nuclear Fusion, **49**, 055004 (2009)

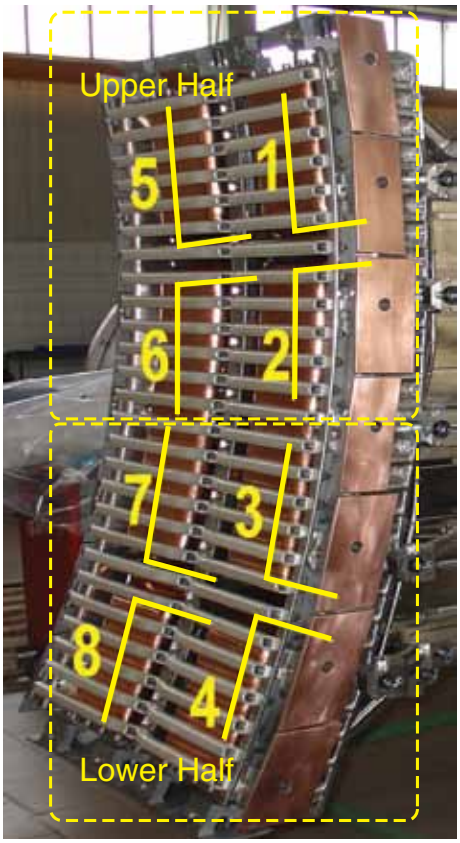

Figure 1: (a) Photo of the ILA antenna before being mounted in JET. Clearly visible are the 8 separate short straps, numbered 1 to 8. Straps (1,2) (3,4) (5,6) and (7,8) are combined into 4 Resonant Double Loops (RDLs), each with a corresponding adjustable capacitor (C1 to C8, not visible). The 'upper half' refers to RDLs (1,2) and (5,6). The 'lower half' to RDLs (3,4) and (7,8).

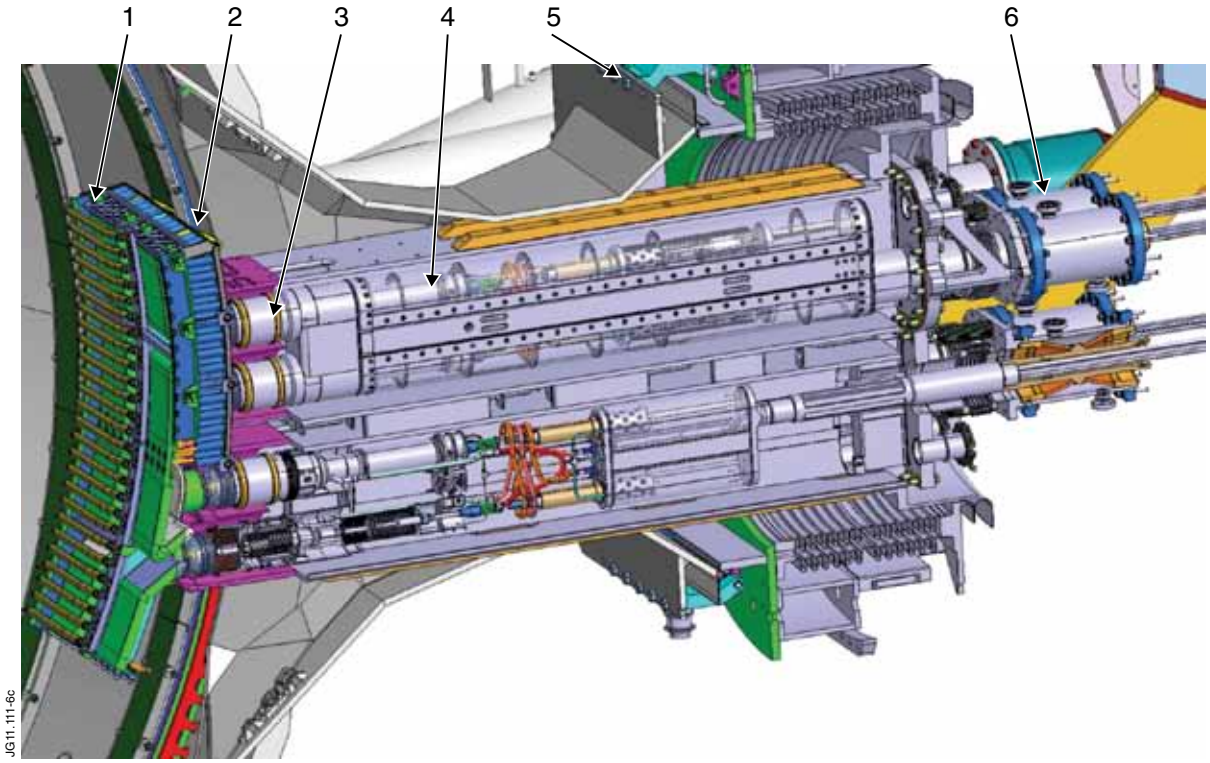

Figure 1: (b) Schematic cut-out view of the ILA : 1) antenna straps in antenna housing, 2) antenna housing, 3) matching capacitors, 4) low impedance vacuum transmission line which is quarter wave long a mid-band frequency with a characteristic impedance of 9 Ohm : this transforms the 3 Ohm impedance of the C_T to 30 Ohms of the feeding transmission lines, 5) JET's port flange, 6) Vacuum Ceramic Windows.

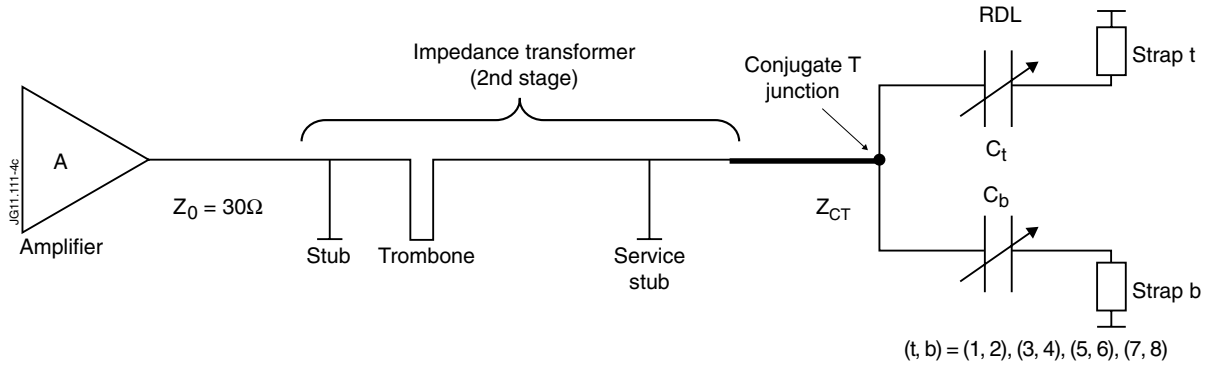

Figure 1: (c) Schematic of the load resilient RF circuit of as realised in the ITER Like Antenna (ILA). The 8 straps of the ILA as illustrated in Fig. 1e are combined into Resonant Double Loops (RDL) in a Conjugate T junction (C_T). A variable capacitor (located inside vacuum) is adjusted such that the two branches of the RDL have a conjugate complex impedance. An impedance transformer (also called 2nd stage matching circuit) adapts the low impedance Z_{CT} to the impedance Z_0 of the transmission line connected to the amplifier output.

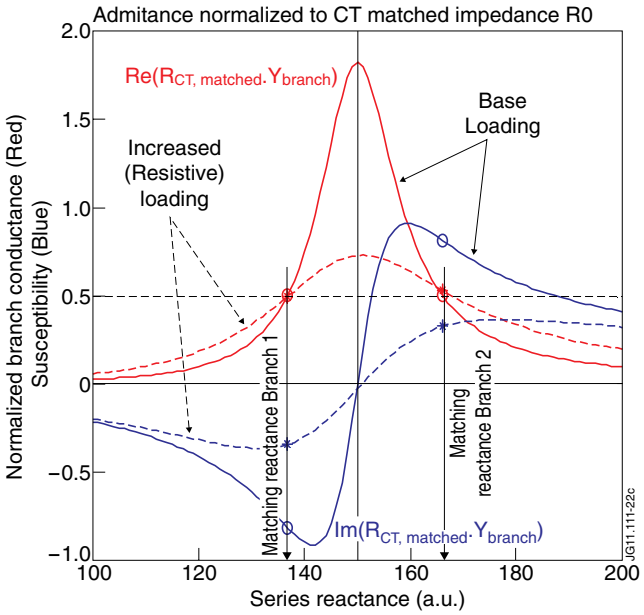

Figure 1: Conjugate-Tee matching principle for the ILA : a capacitive reactance is added to each of the two straps which have an inductive reactance thus forming the two branches which are combined at the T-junction. The normalized branch admittances (real conductance (red) and imaginary susceptibility (blue)) are shown as a function of the added capacity for a normal loading case (plain lines) and a ELM like loading case (dashed lines). For the appropriate normalization impedance the sum of the conductances appearing at parallel connection of the two branches will vary little while the sum of the susceptibilities will keep cancelling. Therefore the circuit exhibits a load resilience.

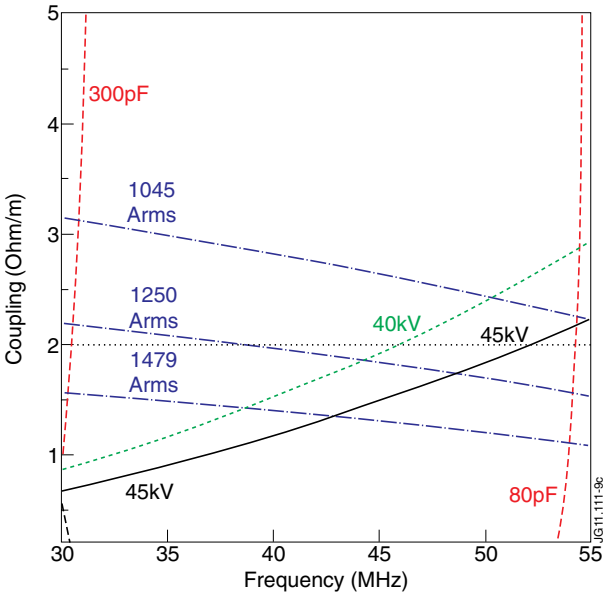

Figure 1: Operational domain bound by the capacitor range (80 to 300 pF), Antenna strap and Capacitor currents (nominally 1250 Arms for 10s) and Capacitor and Feeder voltages (target 45kV).

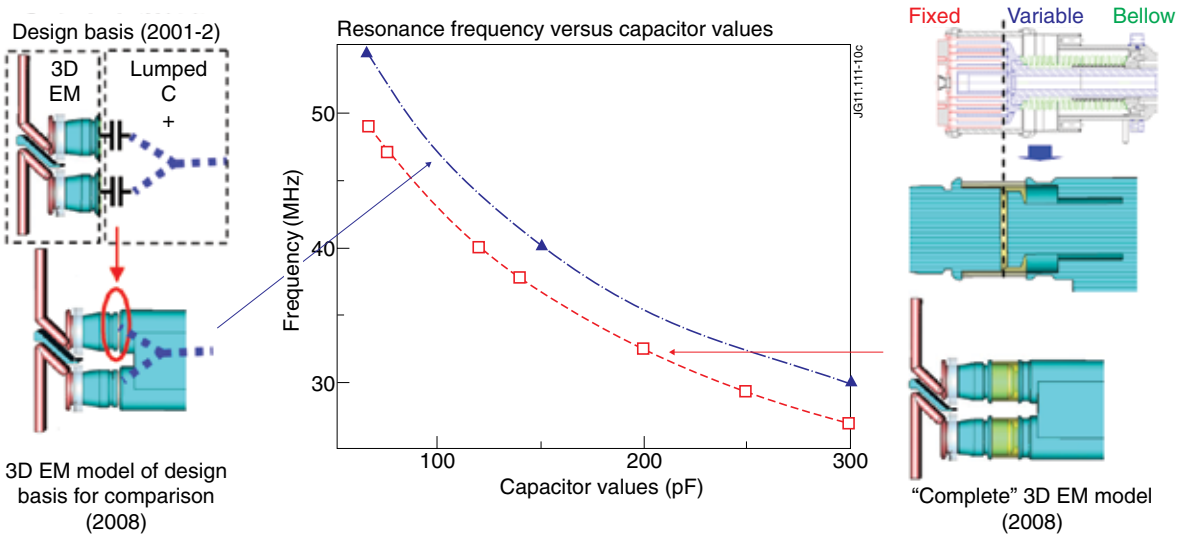

Figure 4: Explanation of the ILA upper frequency band deficiency. (left upper) the model used for the design evaluation : a 3D model of the antenna housing and straps with a lumped / transmission line circuit model of the matching capacitors and feeding VTL. (left lower) the model made in 2008 to compare with a more detailed model of the capacitor shown in right lower : the capacitor itself if modelled as a dielectric slab with an permittivity so as to correspond to the capacitor value required. (middle) the results of the modelling of the RDL circuit resonance frequency vs. the value of the capacitor for both models left lower and right lower : blue triangles : original modelling performed with model shown to the left, red squares : revised modelling performed with model shown to the right. (right upper) detailed drawing of a real capacitor showing the reference plane where the capacitor is located in the circuit. (right middle) the capacitor used in the more recent modeling of the ILA : as with the model in the left lower the capacitor is modeled as a dielectric slab. (right lower) complete model of the RDL with the more accurate capacitor model.

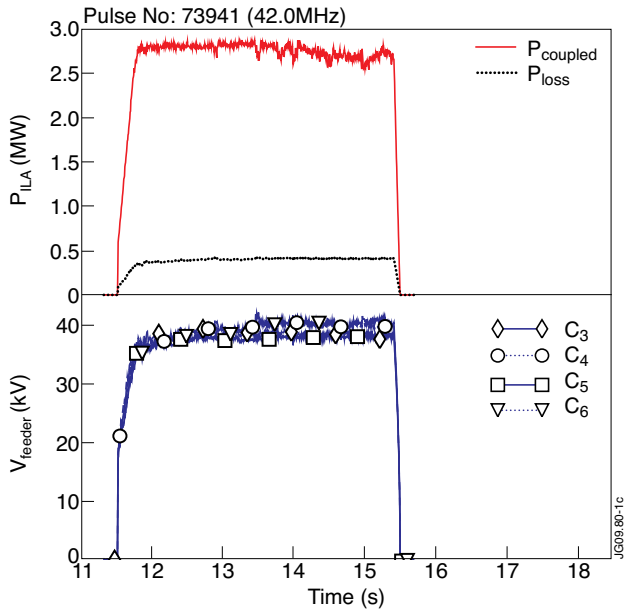

Figure 5: JET Pulse No: 73941 Highest power density in L-mode. Coupled power is measured at the Antenna Pressurized Transmission Line (APTL) directional couplers with power losses subtracted. The power losses are estimated using the reactive parts of the ILA impedance matrix measured on testbed to estimated the amplitude of the strap currents and assuming 65mW series resistor per strap representing the losses (as measured on vacuum on the testbed [26]).

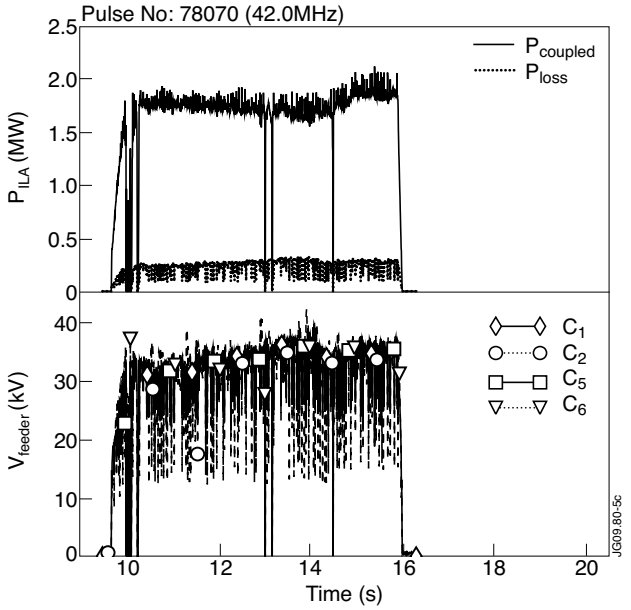

Figure 6: (a) JET Pulse No: 78070 on the ILA upper half.

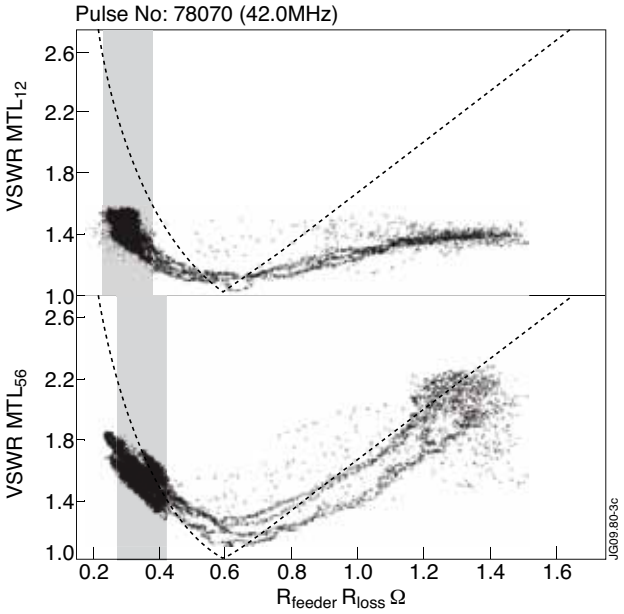

Figure 6: (b) Coupling data for a small time slice for RDL (1,2) and (5,6) for the pulse of Fig. 6a.

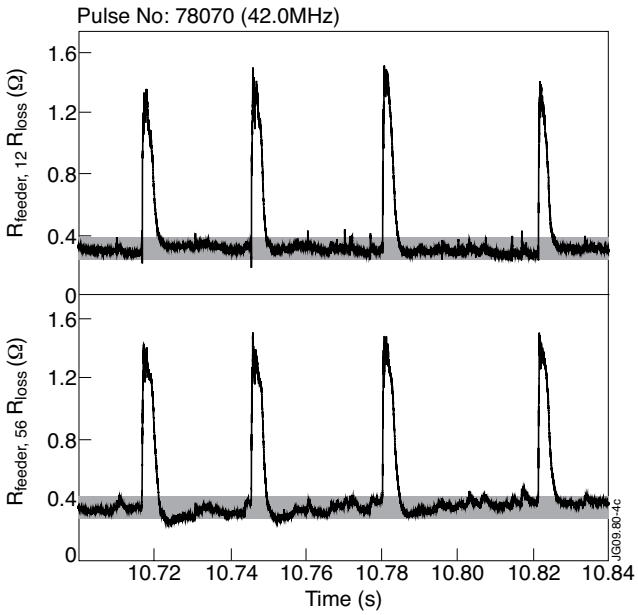

Figure 6: (c) VSWR versus the estimated coupling for the shown time slice in Fig.6b: the dashed line represents what a classic 2-port matching circuit would achieve; the shaded areas correspond to the base load also highlighted in figure 6b.

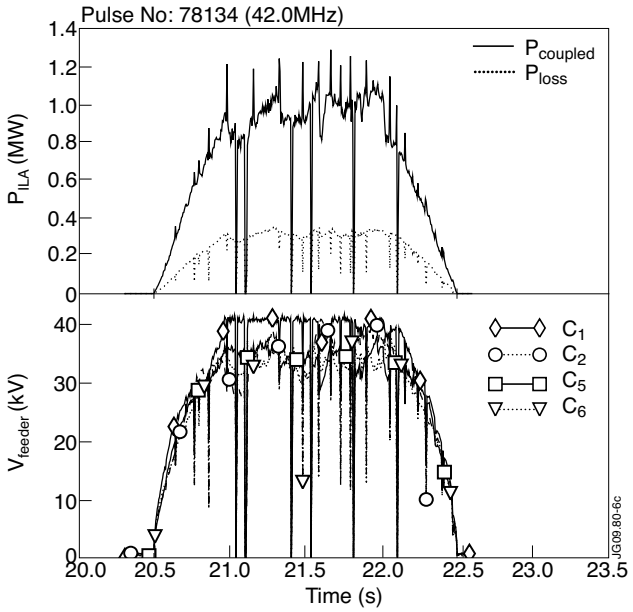

Figure 7: JET Pulse No: 78134. The feeder voltage on strap 1 (C1) is limited at ~42kV limiting the power output of the amplifiers on this pulse with strong ELMs. During the ELMs, when the strap voltage is lower, the power output is raised to the requested value.

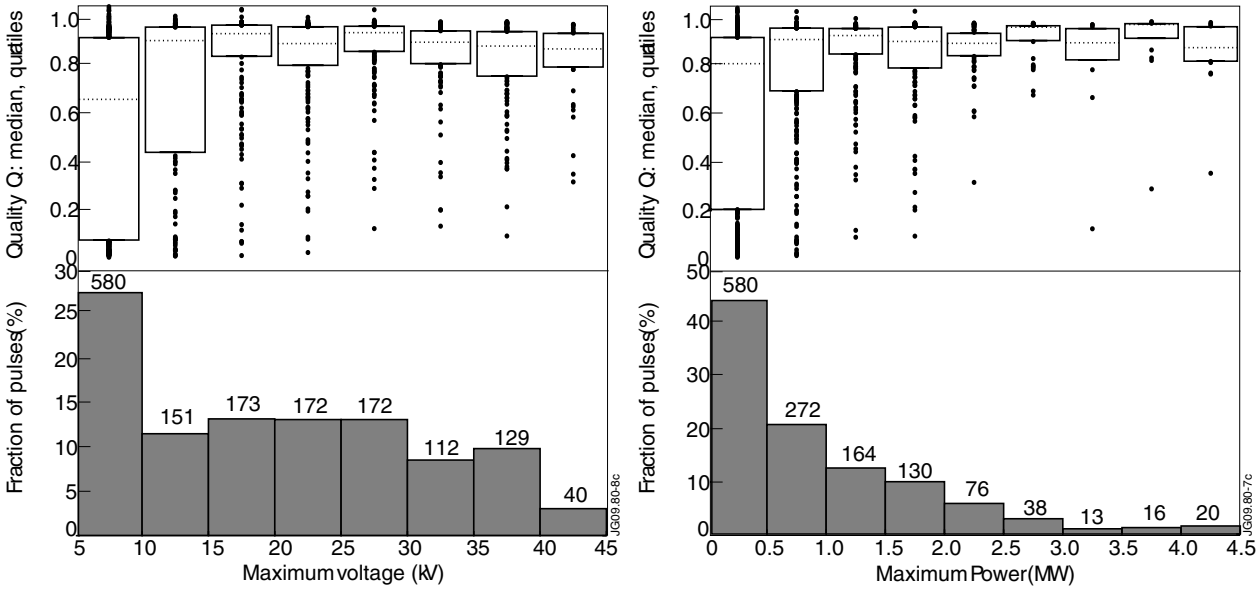

Figure 8: Statistics on achieved voltages (a) and powers (b). The bottom graphs show the distribution of the number of pulses versus voltage/power also showing the number of pulses in each voltage/power bracket. The top graphs show the quality factor Q, defined as the ratio of the delivered to the requested energy when the former has reached 97% of its total, for the pulses in each bracket: 50% of the pulses lie in the inter quartile's box while 50% of the pulses lie above the dotted median line shown in the box. The pulses lying outside of the inter quartile's box are also shown.

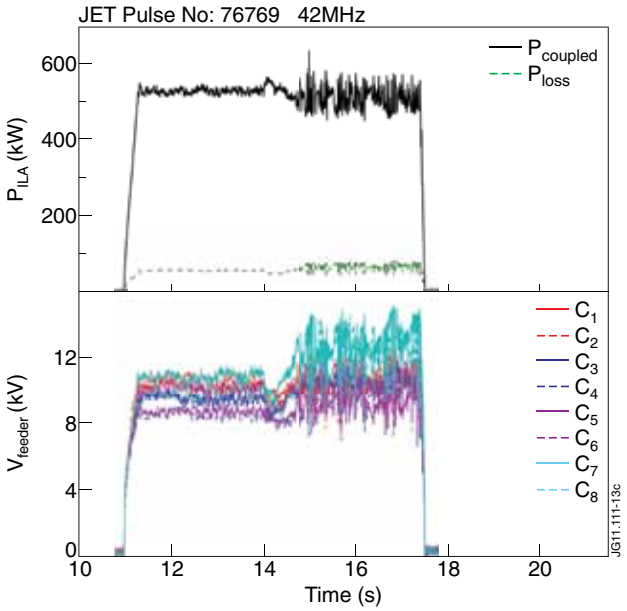

Figure 9: ILA full array operation during and L-H mode transition (14.5s) and subsequent ELMy H-mode plasma.

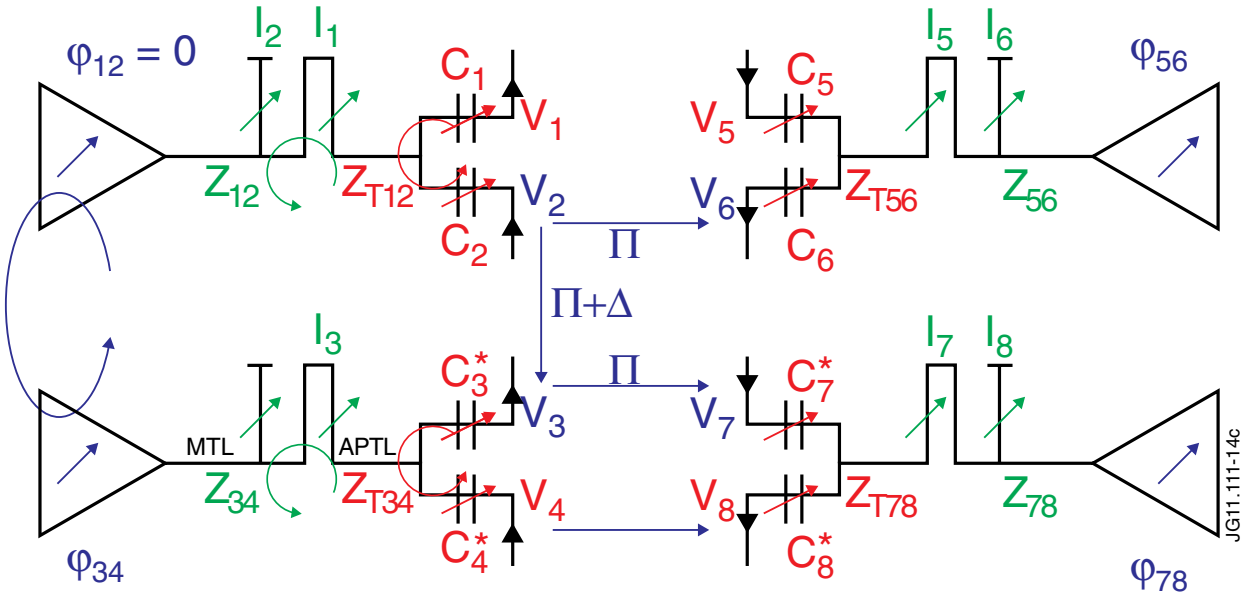

Figure 10: Overview of JET-ILA ICRF matching feedback control system in its final version.

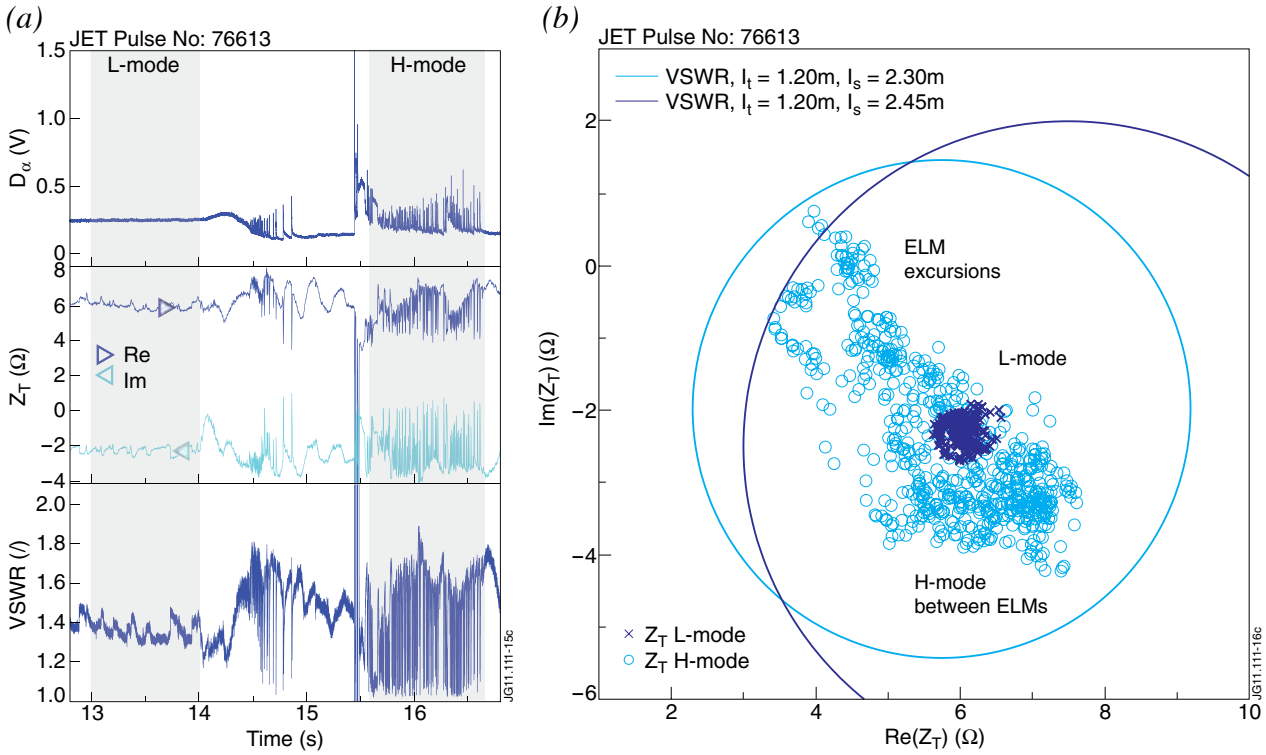

Figure 11: (a) Time evolution of D_α ELM signal, ZT and VSWR during L-mode and ELMy H-mode on JET Pulse No. 76613. (b)Measured T-point impedance during L-mode (13-14s) and ELMy H-mode (15.7-16.7s) in the complex plane with overlaid circles of VSWR = 2.0 for two sets of length l_t, l_s.

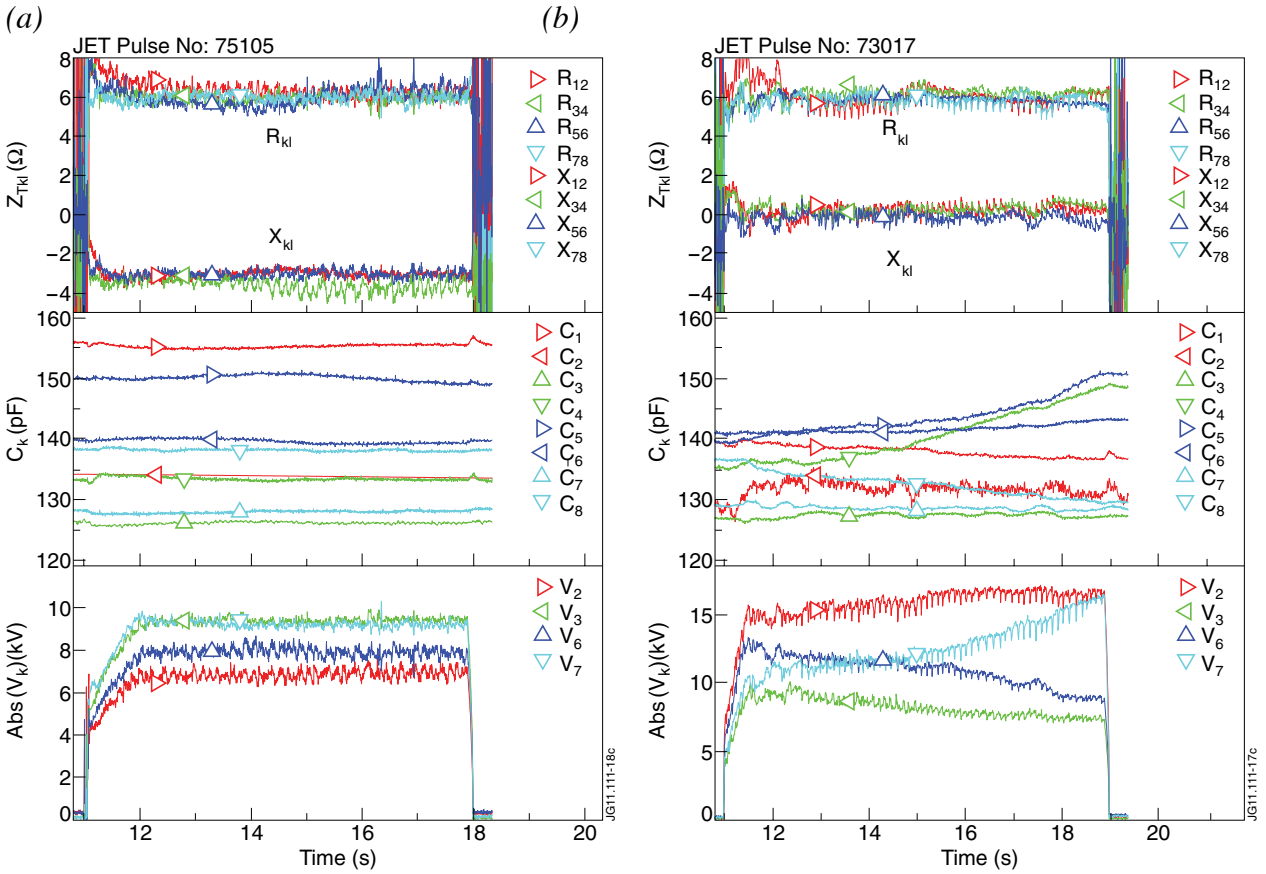

Figure 12: Time evolution of T-point impedances ZT,kl, capacitor values C_k and voltages V_k on (a) JET Pulse No. 73017 without inner strap phase control and (b) JET Pulse No. 75105 with inner strap phase control.

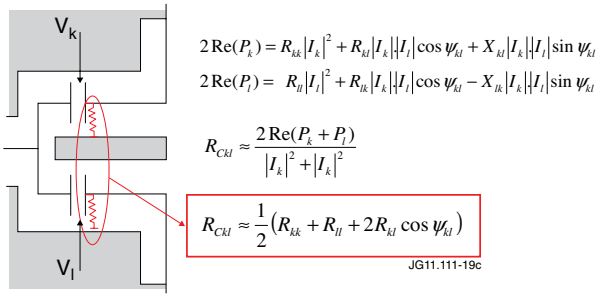

Figure 13: Definition of effective resistive loading R_C,k_l at the capacitor probe position in a Resonant Double Loop (RDL) of the ILA.

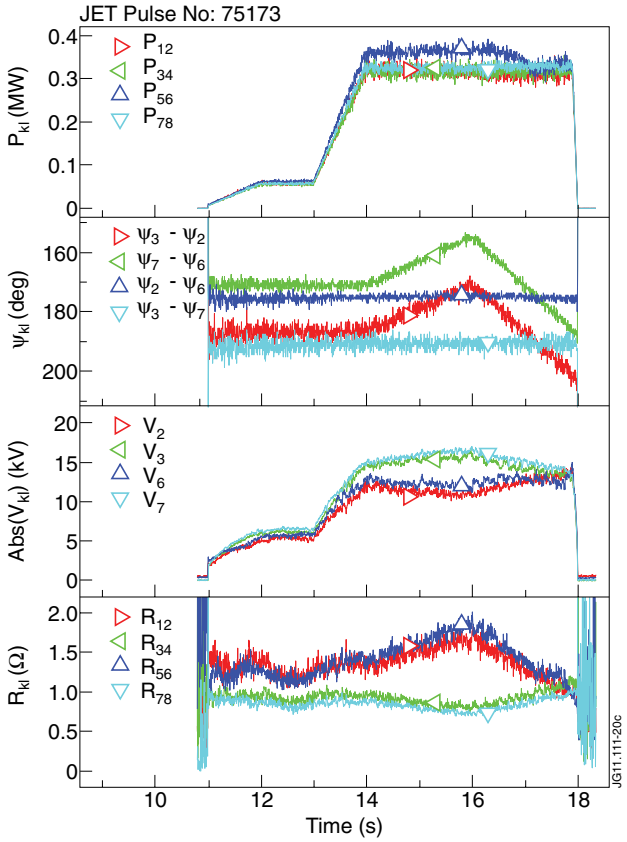

Figure 14: Time evolution of forward power, inner strap phase difference, capacitor voltage and effective load resistance on JET Pulse No. 75173.

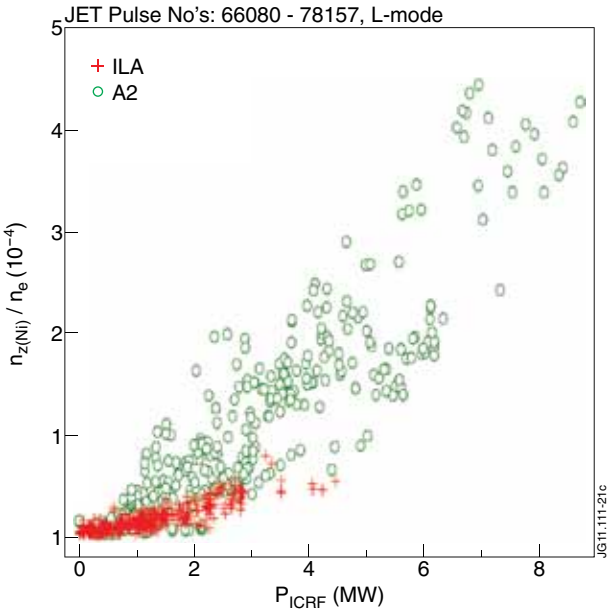

Figure 15: Correlation between Ni concentration ($r/a \approx 0.5$–0.6) obtained with the horizontal VUV spectrometer (KT2) [28] for the ILA (+) and the four A2 (o) antennas as function of the total ICRF power applied.

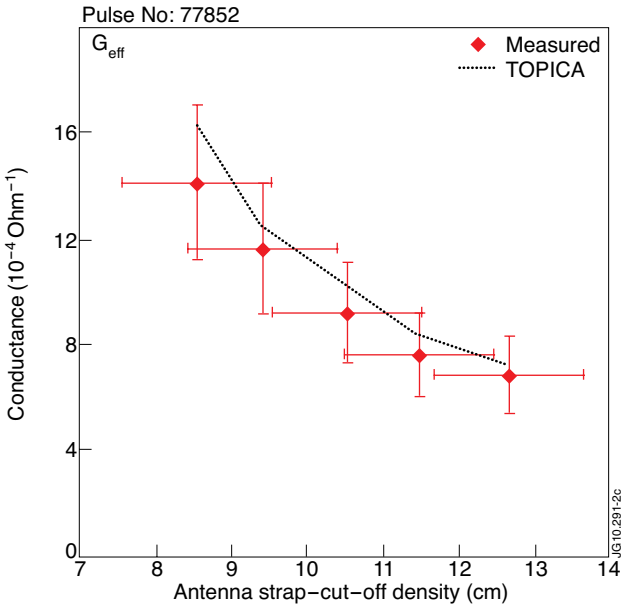

Figure 15: Comparison of the measured and predicted coupling as represented by G_{eff} (a proportionality constant between the power coupled and the square of the system voltage).

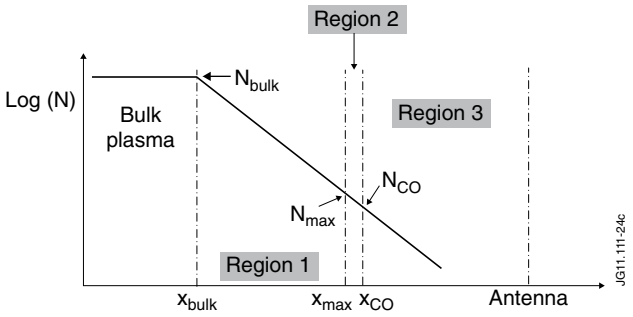

Figure 17: Schematic plot of the density profile in front of the antenna (logarithmic Y-axis) showing the different zones that control the coupling to the bulk plasma: (i) region 3 from the location of the antenna to the cut-off density N_{CO}; (ii) region 2 between the location of N_{CO} and the location of N_{max}, equal to a few times N_{CO}, and defined as the density for which the coupling is maximum in presence of a single step density profile in front of the antenna; (iii) region 1 between N_{max} and N_{bulk}. Coupling is very sensitive to the density gradient in region 1 and to the width of region 2 [45].